J Solid State Electrochem (2008) 12:1151–1157
DOI 10.1007/s10008-007-0463-5

ORIGINAL PAPER

Electrolytic molybdenum sulfides for thin-layer lithium power sources

E. Shembel · R. Apostolova · I. Kirsanova · V. Tysyachny

Received: 20 September 2007 / Revised: 24 October 2007 / Accepted: 24 October 2007 / Published online: 27 November 2007

Abstract The active molybdenum sulfide compound Mo_2S_3, which should be considered as a cathode material for thin-layer rechargeable power source, has been produced by electrolysis. Using impedance spectroscopy and potential relaxation method after current interruption, the kinetic parameters of lithium intercalation in electrolytic Mo_2S_3 have been obtained. Activation energy of Li^+ migration in electrolyte (13.76 kJ/mol), charge transfer through the Mo_2S_3 electrode/electrolyte interface (38.8 kJ/mol), and Li^+ diffusion in a solid phase (57.3 kJ/mol) have also been established. Taking into account the coefficient data of charge mass transfer in a solid phase and the reaction rate coefficient of charge transfer through the interface electrode/electrolyte within the temperature range 20–50 °C, the stage of Li^+ transfer in a solid phase has been determined as a limiting stage for lithium intercalation in electrolytic molybdenum sulfide Mo_2S_3.

Keywords Secondary thin-layer Li cell · Electrolytic molybdenum sulfides · Kinetic parameters

E. Shembel · R. Apostolova · I. Kirsanova
Ukrainian State Chemical Technology University,
Dnepropetrovsk 49005, Ukraine

E. Shembel (✉)
Enerize Corporation, Inc.,
Coral Springs, FL, USA
e-mail: shembel@onil.dp.ua

V. Tysyachny
National Metallurgical Academy,
Dnepropetrovsk, Ukraine

Introduction

Growing demand for autonomous high-energy power sources used in electronic devices has lead to efforts aimed at increasing the efficiency of rechargeable lithium chemical power sources. The electrochemical activity of electrode materials in such power sources depends both on the materials selected and the methods used in their synthesis. Electrolysis methods present a large parameter space in which the systematic variation of chemical composition, morphology, physicochemical, structural, and electrochemical characteristics of electrode materials can be carried out. Electrolysis enables production of thin-layer nonballast electrodes based on the oxides of transition metals such as V, Mn, Mo, Ni, etc., and sulfides of metals such as Fe and Mo, all of which are good candidates for use in thin-layer lithium batteries [1–5].

Electrolytic molybdenum oxide and sulfide composite (e-Mo,OS) were synthesized in compact layers and used as the cathodes of lithium thin-layer batteries [6]. E-Mo,OS (10 mg/cm^2 on 10 μm aluminum substrate) was produced by cathode reduction of a sodium molybdate water solution in the presence of sodium thiosulfate [7]. Physicochemical structural properties of e-Mo,OS were investigated by profilometry, thermal analysis, and IR-spectroscopy methods [8]. Based on data from X-ray diffraction and atomic force microscopy, e-Mo,OS compounds are mainly nanostructured materials, consisting of sulfides (Mo_2S_3, MoS_2, Mo_3S_4) and Mo–oxide admixtures. The aggregate properties of the deposited material depend on electrolyte composition, substrate composition, electrolysis parameters, and thermal treatment. Reversible capacity of e-Mo,OS

ranges from 150 up to 200 mAh/g (depending on the deposit mass) in lithium cell models with liquid [ethylene carbonate (EC), dimethyl carbonate (DMC), 1 M $LiClO_4$] and PVdF-based polymer electrolytes.

Thin-layer e-Mo,OSs are excellent candidates for electrode kinetics investigations, as shown in [8]. The values of the coefficient of ion interaction and ion interaction energy and the lithium ion chemical diffusion coefficient for electrochemical intercalation in electrolytic molybdenum sulfide e-MoS_2 have been determined from cyclic voltammograms.

In this work, investigations of electrode kinetics of electrolytic molybdenum sulfides were carried out using the potential relaxation method (PRM) after current interruption, and by the electrochemical impedance spectroscopy (EIS) technique.

Experimental

Aspects of the synthesis of electrolytic molybdenum sulfide compounds

Molybdenum sulfides were deposited by cathode reduction of aqueous solutions of sodium molybdate and nickel sulfate (total concentration is 0.08–0.14 mol l^{-1}) with sodium thiosulfate (0.01–0.012 mol l^{-1}). Stable electrolysis conditions were reached at an electrolyte temperature of 85±3 °C, $I_{cathode}$=3.5–7.5 mA cm^{-2}, $S_{cathode}$:S_{anode}=1:5, pH=5.0–6.0. The synthesized materials were produced as compact deposits with the mass of 1–12 mg cm^{-2} on a foil (25–100 μm thickness) of the aluminum alloy AMG-6. Smooth plates of technical-grade titanium (VT-1) were used as anodes. Electrolytic deposits were subjected to thermal treatment at 180 °C for 7 h.

Cathode production of molybdenum sulfides can occur according to different mechanisms. The overall process of molybdenum disulfide formation may be described by the following equations [9]:

$$MoO_4^{2-} + S_2O_3^{2-} + 14H^+ + 10\bar{e} \rightarrow MoS_2 + 7H_2O \quad (1)$$

$$Mo_2O_3 + 3S^{-2} + 6H^+ \rightarrow Mo_2S_3 + 3H_2O \quad (2)$$

$$3MoO_2 + 4S^{-2} + 12H^+ + 4\bar{e} \rightarrow Mo_3S_4(Mo_2S_3 * MoS) + 6H_2O \quad (3)$$

Investigation of lithium intercalation in molybdenum sulfides

Electrochemical parameters of molybdenum sulfides during galvanostatic discharge–charge processes were investigated at room temperature in a lithium test cell with thin-layer e-Mo,OS cathodes, lithium anodes, and a Li/Li^+ reference electrode. The models were filled with a liquid electrolyte comprising 1 M $LiClO_4$ (Iodobrom, Crimea, Ukraine), propylene carbonate (PC, Angarsk Chemical Reagent Plant, Angarsk, Russia), dimethoxyethane (DME, Merck, Whitehouse Station, NJ, USA) in the volume ratio 1:3, and PVdF-CTFE (31508/1001 Solvay), EC, DMC (Merck), and 0.5 M $LiClO_4$ polymer electrolyte.

Potential relaxation method

The method proposed in Wang et al. [10] enables $\widetilde{D}_{Li}$ determination at different stages of molybdenum oxysulfide discharge based on the mathematical diffusion model describing the behavior of a flat intercalated electrode after charge/discharge process interruption. The Li/1 M $LiClO_4$, PC, DME/e-Mo,OS system was the object of the present investigation.

Electrochemical impedance spectroscopy technique

Impedance spectra were determined for the system of e-Mo, S-electrode–electrolyte–e-Mo,S in the four-electrode Li–e-Mo,S–e-Mo,S–Li model as a function of electrolyte temperature and e-Mo,S-electrode intercalation degree. The two identical working e-Mo,S electrodes, with 1×1 (cm) geometrical area were sulfur-containing materials with the mass of 1.5–3.0 mg/cm^2, produced on a stainless steel gauze. On both of the e-Mo,S electrodes, there were 1×1×0.01 (cm) size Li electrodes. They were used for changing the degree of discharge of the e-Mo,OS-electrode. In this battery model, electrodes are divided into 100–300-μm electrolyte layers. With the help of an analytical radiometer (VoltaLab PJZ 301), the impedance spectrum of the system e-Mo,S–electrolyte–e-Mo,S was determined by applying a 10-mV-amplitude electrical signal within the frequency range from 100 kHz to 4 mHz. For registration and analysis of the impedance spectra, the programs ZPlot and ZView (version 2.1b) were used. Application of gauze to the thin-layer e-Mo,S electrodes enabled their homogeneous polarization. Before impedance measurement, the investigated system was equilibrated without current for 15 h. In that case, the sulfide electrode potential corresponded to the open circuit potential near equilibrium at the intercalation degree (E_{0CV}). During a pause, e-Mo,S electrodes were short circuited to achieve equipotentiality.

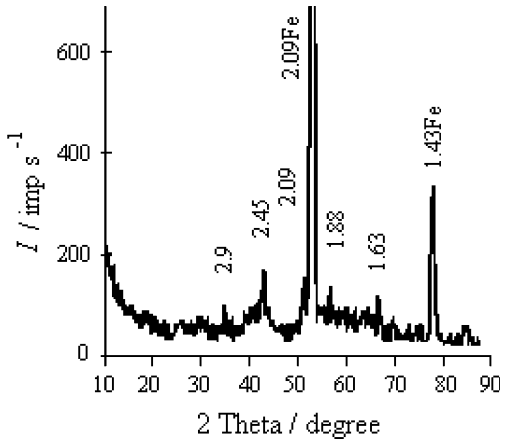

Fig. 1 X-ray pattern of e-Mo_2S_3 synthesized on stainless steel. Co – K_α radiation

Results and discussions

Determination of lithium chemical diffusion coefficient in e-Mo_2S_3 by the PRM

As determined by X-ray phase analysis, the structure of investigated material corresponds to the molybdenum sulfide Mo_2S_3 structure (ICPDS 12–693)—Fig. 1. The open circuit voltage (OCV) of the e-Mo, S/Li system is 3.45–3.60 V. A hysteresis-type profile obtained upon system cycling is shown in Fig. 2. In the first cycle, the discharge profile differs from those obtained in the second and subsequent cycles. In the first discharge process, voltage changes monotonically from 2.8 up to 1.45 V; then the slope of curve changes, whereupon monotonic voltage drop continues again up to 1.1 V. In the second cycle, a sloping voltage plateau takes place, and a voltage drop within the range of 1.8–1.1 V occurs uniformly. In the second cycle, the initial discharge capacity (340–370 mA h^{-1} g^{-1}) decreases by 20% upon cycling within the range of 2.9–1.1 V. Reversible capacity ranges within about 200 mA h^{-1} g^{-1}.

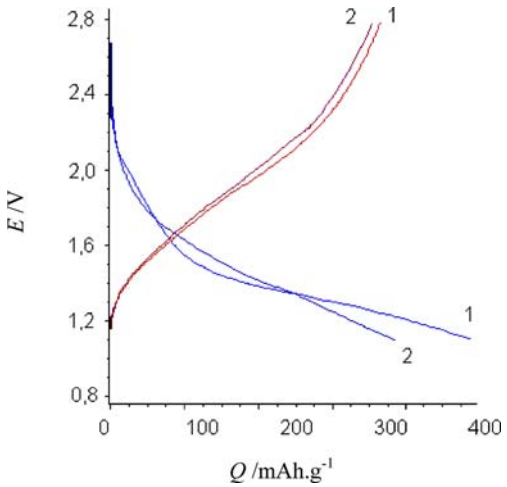

Fig. 2 Discharge–charge profile of the model based on e-Mo_2S_3. Mass: 3.3 mg/cm^2 Electrolyte: PC, DME, 1M $LiClO_4$. *I*disch= 0.05mA.cm^{-2}, *I*charg=0.03mA.cm^{-2}

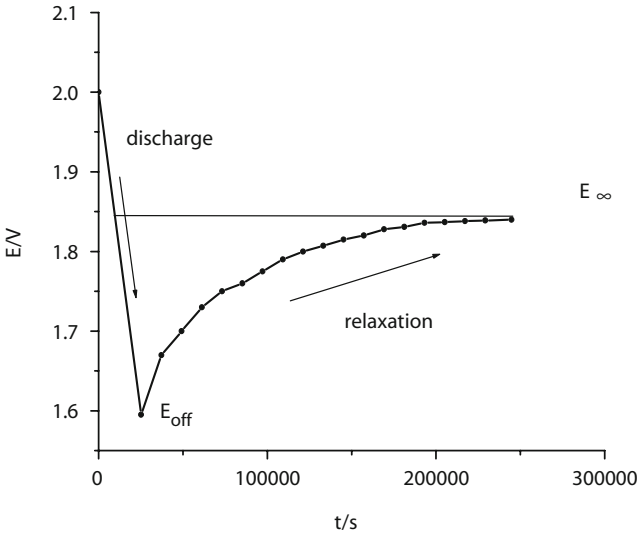

Fig. 3 General view of potential relaxation curve after current switched off in the model of e-Mo_2S_3/PC, DME, 1 M $LiClO_4$/Li. *I*disch=0.05 mA cm^{-2}, *l*=13.3.10^{-4} cm

At the relaxation time $t \gg l^2/(\pi^2 * \widetilde{D}_{\mathrm{Li}})$, the $\widetilde{D}_{\mathrm{Li}}$ value is obtained by the method of Wang et al. [10], based on the relaxation curve (Fig. 3) by the slope of its linear portion at the coordinates $\ln\left[\exp\left(\frac{E_\infty - E(l,t)}{\frac{RT}{F}}\right) - 1\right]$ relatively to *t*:

$$\widetilde{D}_{\mathrm{Li}} = -\frac{l^2 \mathrm{tg}\alpha}{\pi^2}, \tag{4}$$

where *l* is the electrode thickness; $\widetilde{D}_{Li}$ is the lithium chemical diffusion coefficient in a solid phase, and E_∞ is the electrode potential as $t \to \infty$.

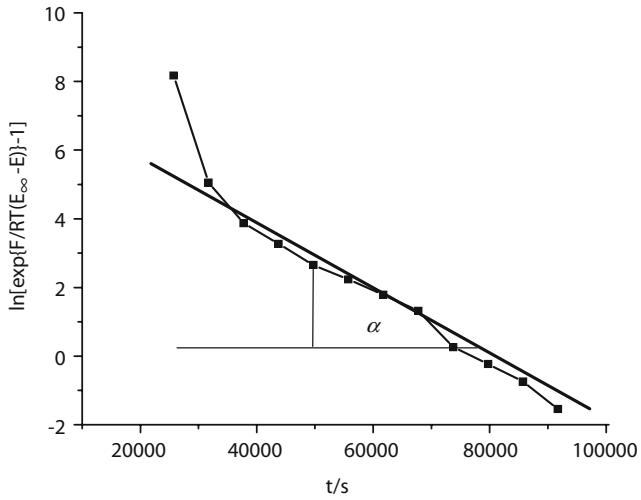

Fig. 4 Relaxation curve at lg [exp(*F*/*RT*(*E*∞-*E*))-1] vs *t* coordinates

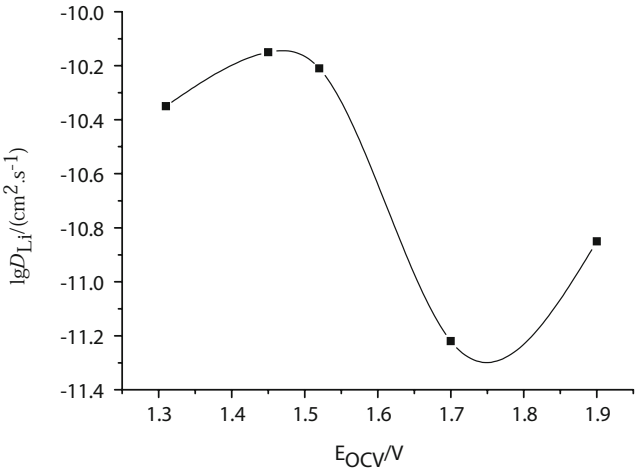

Fig. 5 Dependence of Li^+ chemical diffusion coefficient ($\widetilde{D}_{Li}$) on potential in e-Mo_2S_3

Figure 3 shows the potential relaxation curve for the case wherein the discharge current is turned off at E_{off}=1.59 V. The relaxation curve at the coordinates $\ln[\exp(F/RT(E_\infty - E)) - 1]$ relative to t as obtained from Fig. 3 is shown in Fig. 4. From the linear part of the relaxation curve, the value of tg α=0.8*10^{-4} c^{-1} was obtained. The $\widetilde{D}_{Li}$ value calculated by Eq. 4 for this case is equal to 1.44*10^{-11} cm^2 s^{-1}. The dependence of lg $\widetilde{D}_{Li}$ on the open circuit potential (E_{OCV}) is shown in Fig. 5.

Within the potential range of E_{OCV}=1.9–1.3 V, the change in $\widetilde{D}_{Li}$ takes place nonlinearly. The order of magnitude for the $\widetilde{D}_{Li}$ values obtained for e-Mo_2S_3 by the PRM agree well with those established by the method of cyclic voltammetry [8].

Kinetic parameters of lithium intercalation in e-Mo_2S_3 established by EIS method

As depicted in a Nyquist diagram, the impedance spectrum of the e-Mo_2S_3/PVdF, EC, DMC, 1 M $LiClO_4$/e-Mo_2S_3 system with molybdenum sulfide discharged up to 1.1 V vs Li/Li^+(E_{0CV}=1.32 V), is a compressed semicircle converted into a line (Fig. 6).

Changes in the impedance spectra of the system as a function of temperature (293, 307, 319, and 332 K) are shown in Fig. 7. The structure of the impedance spectrum is altered by changing temperature. The impedance of the system increases with decreasing temperature both in the high-frequency regime and in the low-frequency linear range. The spectra were analyzed with the help of selected analog circuits. The impedance spectra and the analog circuit of the system and its functional parameters are shown in Fig. 6 for T=293 K.

With the help of the Arrhenius equation, which can be presented in general as

$$\frac{\mathrm{dlg}A}{\mathrm{d}\left(\frac{1}{T}\right)} = -\frac{E}{RT}, \tag{5}$$

values for the activation energy (E) were calculated from the experimental data. The activation energy (E) is the energy associated with lithium ion migration in the electrolyte, or the activation energy of lithium ion transfer through the electrode/electrolyte interface, where A is the electrolyte conductivity "σ," or exchange current i_0.

Parameters $R1$ and $R2$ established by EIS are accepted as determinative to obtain electrolyte resistance and the

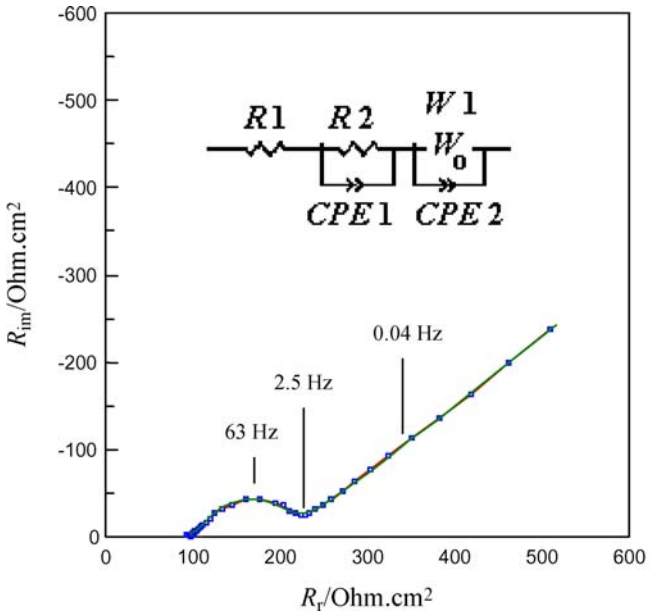

Parameter	Value	Error, %
$R1$/Ohm.cm^2	95,79	0,79
$R2$/Ohm.cm^2	83,61	2,37
$CPE1$-T/F.cm^{-2}	7,37·10^{-5}	2,13
$CPE1$-P/F.cm^{-2}	0,85	3,31
$W1$-R/Ohm.s$^{-1/2}$	94,64	2,67
$W1$-T/Ohm.s$^{-1/2}$	0,91	1,3
$W1$-P/Ohm.s$^{-1/2}$	0,21	1,66
$CPE2$-T/F.cm^{-2}	1.6·10^{-6}	11,28
$CPE2$-P/F.cm^{-2}	0,96	5,89

Fig. 6 Impedance spectrum of e-Mo_2S_3/PC, DME, 1 M $LiClO_4$/e-Mo_2S_3 system and parameters of equivalent circuit (frequency: 100 kHz–6.3 mHz). T=293 K

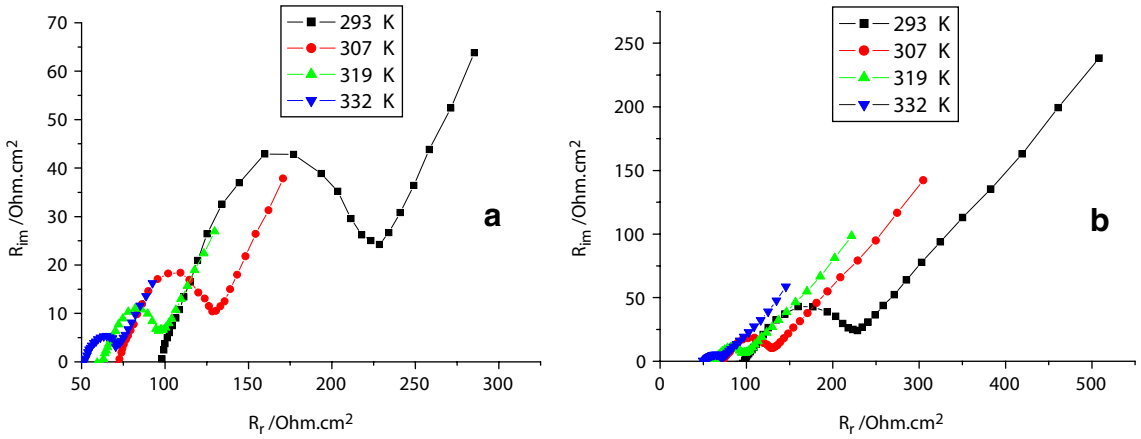

Fig. 7 Impedance spectrum of e-Mo_2S_3/PC, DME, 1 M $LiClO_4$/e-Mo_2S_3 system depending on temperature: **a** frequency: 100 kHz–0.15 Hz, **b** frequency: 100 kHz–6.3 mHz

resistance of charge transfer though the electrode/electrolyte interface, respectively. For determination of the activation energy of lithium ion migration in electrolyte (E_e), and activation energy of lithium ion transfer through the electrode/electrolyte interface (E_{ct}), the data from Figs. 8 and 9 have been used, respectively.

The current exchange values of Li^+ transfer through electrode/electrolyte interface are calculated from the data obtained by impedance spectroscopy for charge transfer resistance R_{ct}:

$$i_o = \frac{RT}{FR_{ct}} \tag{6}$$

where R_{ct} is the charge transfer resistance in ohms per square centimeter; i_o is the exchange current, in A/cm^2; and T is the temperature in K. The others parameters have conventional values.

From the slope of straight portions of Figs. 8 and 9, the following values have been calculated: E_e=13.76 kJ/mol and E_{ct}=38.8 kJ/mol at E_{ocv}=1.32 V.

From Eqs. 7 and 8, the lithium ion chemical diffusion coefficient $\widetilde{D}_{Li}$ and the activation energy of lithium ion diffusion in solid phase E_a of molybdenum sulfide e-Mo_2S_3 have been obtained:

$$\widetilde{D}_{Li} = \left(\frac{l\left(\frac{dE_p}{dx}\right)}{\sqrt{2}\cdot Q_m A_w} \right)^2, \tag{7}$$

$$E_a = -2.3R\frac{d\lg D}{d(1/T)} \tag{8}$$

where E_a is the activation energy of lithium ion diffusion in solid phase, in joules per mole; l is the thickness, in centimeters; Q_m is the maximum electrode capacity, in coulombs per square centimeter; A_w is the Warburg constant, ohms per square centimeter per root second ($S^{-1/2}$); and dE_p/dx is derivative of equilibrium electrode potential by the intercalation degree, in volts.

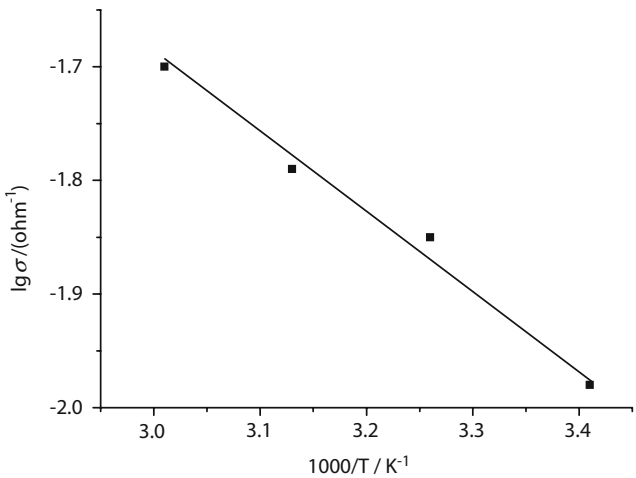

Fig. 8 Dependence of electrolyte conductivity (σ) on temperature (T). PC, DME, 1 M $LiClO_4$

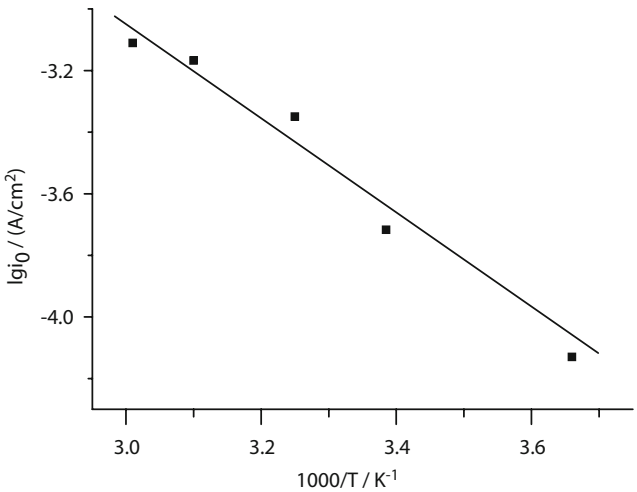

Fig. 9 Dependence of exchange current (i_0) on temperature (T). E_{OCV}=1.32 V

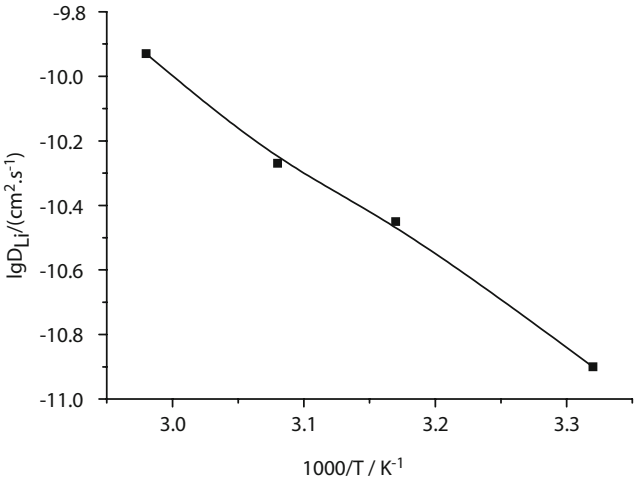

Fig. 10 Dependence of chemical diffusion coefficient ($\widetilde{D}_{\mathrm{Li}}$) on temperature ($T$) in e-$Mo_2S_3$

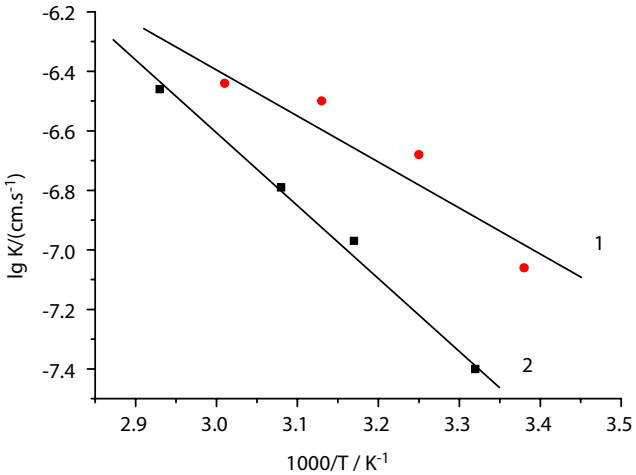

Fig. 12 Dependence of K_s (*1*) and K_g (*2*) constants on temperature (T)

On the linear section of the impedance spectrum characterizing lithium ion diffusion in a solid phase within the frequency range of 100–4 mHz, there is a frequency interval where the slope is equal to 45°. The Warburg constant A_w was determined by the slope of this line section.

The dE/dx value was determined from the $E_{0\mathrm{CV}}$ dependence on x. The electroactive material thickness is l=13.3 μm. Experimental dependence of the lithium ion chemical diffusion coefficient on temperature in the investigated material is shown in Fig. 10. The value of lithium diffusion activation energy in the solid phase e-Mo_2S_3 was calculated with the help of Eq. 8 and the data in Fig. 10 and was determined to be equal to 57.3 kJ mol^{-1}.

The dependence of the chemical diffusion coefficient of $Li^+\widetilde{D}_{Li}$ in the e-Mo_2S_3 solid phase on the potential open circuit (E_{OCV}) for the intercalation process is shown in Fig. 11. The presence of a maximum at the potential corresponding to the peak of the potentiodynamic curves at the potential scanning rate of 10 μV s^{-1} obtained in Shembel et al. [8] is a characteristic feature. Correspondence between the potentiodynamic curve peak and the $\widetilde{D}_{\mathrm{Li}} - E_{(\mathrm{OCV})}$ maximum, in accordance with intercalation theory, shows repulsion of intercalated ions that is characterized by the interaction parameter of g>(−4) [11].

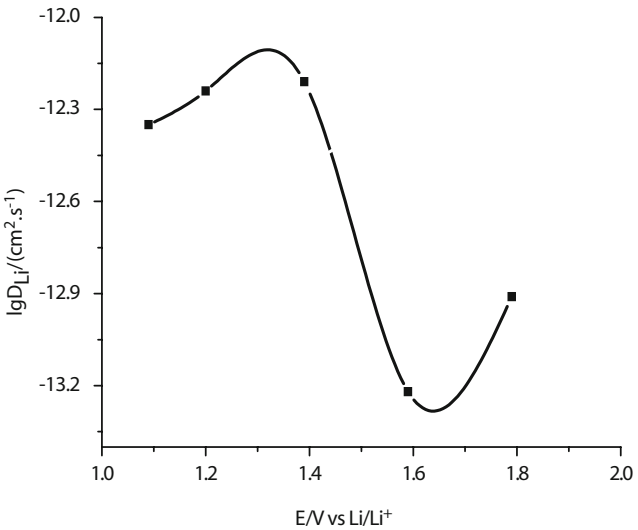

Fig. 11 Dependence of chemical diffusion coefficient ($\widetilde{D}_{\mathrm{Li}}$) on E_{ocv} obtained by EIS

For evaluation of the type of electrochemical process involved in the e-Mo_2S_3 discharge, we abandoned consideration of the current exchange (i_0) in favor of the rate constant characteristic or parameter according to the equation:

$$K_{\mathrm{S}} = \frac{i_0 V}{Q_{\mathrm{m}}[x(1-x)]^{\alpha}}, \tag{9}$$

where K_s is the rate constant in centimeters per second, V is the volume of the intercalation material in cubic centimeters, x is the intercalation degree, and α is the transfer coefficient. In the calculation, α=0.5, x=0.5, Q_m=21.6 C/cm^2, and V=5.10^{-3} cm^3 were used.

For comparison of the rate constant having the dimension of centimeters per second, with the diffusion rate ($\widetilde{D}_{Li}$, cm^2 s^{-1}), we switched from consideration of the diffusion coefficient to use of the mass transfer coefficient, K_g:

$$K_{\mathrm{g}} = \widetilde{D}_{\mathrm{Li}} \Big/ l \tag{10}$$

where K_g is the mass transfer coefficient in centimeters per second, l is the thickness in centimeters, and $\widetilde{D}_{\mathrm{Li}}$ is the Lithium chemical diffusion coefficient in square centimeters per second.

The temperature effect on the coefficient of mass transfer K_g and the rate constant K_s is depicted in Fig. 12. Taking into account the coefficient of charge mass transfer data in the solid phase, and the reaction rate coefficient of charge

transfer through the interface electrode/electrolyte within the temperature range 20–50 °C, the process of Li^+ transfer in a solid phase has been determined as a limiting step for lithium intercalation in electrolytic molybdenum sulfide Mo_2S_3.

Analysis of the possible degradation of the investigated lithium cell model based on e-Mo_2S_3, associated with electrolyte decomposition in the case of polymer electrolyte use, has been carried out. According to impedance spectroscopy data, the resistance of the PVdF-CTFE, DMC, EC, and $LiClO_4$ electrolyte (12 Ohm cm^2) in the model of e-Mo_2S_3/PVdF-CTFE, DMC, EC, and $LiClO_4$/Li with discharge capacity equal to 150 mA h/g increases up to 260 Ohm cm^2 at capacity drop up to 25 mA h/g. The data conform to the electrochemical degradation of the PVdF-CTFE-based polymer electrolyte, resulting in degradation of the e-Mo_2S_3–polymer electrolyte–Li system as a whole. In this case, the essential increase of lithium electrode polarization is determined by lithium contact loss with the electrolyte, whereas microinjection of liquid electrolyte decreases polarization and promotes an increase in discharge capacity in the model. Chemical compatibility of e-Mo_2S_3 with polymer electrolyte and Li during long-term storage is demonstrated.

Conclusion

Electrolytic molybdenum sulfide e-Mo_2S_3 interacts reversibly with lithium in this model of a lithium battery in the 2.9–1.1-V voltage range. Discharge capacity of e-Mo_2S_3/Li (in the first cycle it is 340–370 mA h/g) decreases with cycling. Reversible capacity after 50 cycles is 150–200 mA h/g depending on molybdenum sulfide mass. In the e-Mo_2S_3 solid phase, the value of the lithium ion chemical diffusion coefficient $\widetilde{D}_{Li}$ was determined. Depending on the discharge degree, this parameter value is lower by the EIS method than that obtained by the PRM method. However, the character of the $\widetilde{D}_{Li}$ dependence on the degree of e-Mo_2S_3 discharge (E_{OCV}) is the same (Figs. 5 and 11). The values of the activation energy of lithium ion migration in the electrolyte (13.76 kJ/mol), the activation energy of lithium ion transfer through the interface of the e-Mo_2S_3/electrolyte (38.8 kJ/mol), and that of lithium ion diffusion in the solid phase of e-Mo_2S_3 (57.3 kJ/mol) are compared. From data including the coefficient of charge mass transfer in a solid phase and the reaction rate coefficient of charge transfer through the electrode/electrolyte interface within the temperature range 293–323 K, the process of Li^+ transfer in solid phase has been determined as a limiting step of lithium intercalation in electrolytic molybdenum sulfide.

At investigation, the lithium electrode in the e-Mo_2S_3/PC, DME, 1 M $LiClO_4$/Li system has shown that it does not preclude obtaining satisfactory specific discharge characteristics of the electrochemical system. Discharge capacity decreases with e-Mo_2S_3/Li system cycling in the model of a lithium battery with the polymer electrolyte based on a PVdF-CTFE matrix within the range of 2.9–1.1 V. To a considerable degree, this decrease is driven by polymer electrolyte electrochemical instability.

Acknowledgements The authors acknowledge with thanks the financial support provided of the Ministry of Education and Science of Ukraine (contract 42040290) and Inter Intel. (USA).

References

1. Apostolova RD, Nagyrny VM, Shembel EM (1998) Electrochemistry 34:778(in Russian)
2. Shembel E, Apostolova R, Nagirny V, Aurbach D, Markovsky B (2001) J Power Sources 96:266
3. Shembel E, Apostolova R, Nagirny V (2004) Electrochemistry 40:40(in Russian)
4. Shembel E, Apostolova R, Nagirny V, Baskevich A, Lytvyn P (2004) Electrochemistry 40:821(in Russian)
5. Shembel E, Apostolova R, Nagirny V, Kirsanova I, Grebenkin Ph, Novak P (2005) J Solid State Electrochem 9:96
6. Nagirny V, Apostolova R, Baskevich A, Shembel E (2003) J Appl Chem 76:1477(in Russian)
7. Apostolova RD, Nagirny VM, Kirsanova IV, Bannik NG, Shembel EM Application a 200604872 (UA) 05.03.2006.
8. Shembel EM, Apostolova RD, Tysyachny VP, Kirsanova IV (2005) Russ J Electrochem 41:1305
9. Shembel EM, Nagyrny VM, Apostolova RD (UA), Novak P (US) Patent 67134A (UA)
10. Wang Q, Li H, Huang X, Liquan C (2001) J Electrochem Soc 148:737
11. Levi MD, Aurbach D (1999) Electrochim Acta 45:165